


## Nonmonotonic skewness of currents in nonequilibrium steady states

Sreekanth K. Manikandan<sup>1,\*</sup>, Biswajit Das<sup>2,†</sup>, Avijit Kundu<sup>2,†</sup>, Raunak Dey,<sup>2</sup> Ayan Banerjee,<sup>2,‡</sup> and Supriya Krishnamurthy<sup>3,§</sup>

<sup>1</sup>NORDITA, KTH Royal institute of technology and Stockholm university, Stockholm SE-10691, Sweden

<sup>2</sup>Department of Physical Sciences, Indian Institute of Science Education and Research Kolkata, Mohanpur Campus, Mohanpur, West Bengal 741246, India

<sup>3</sup>Department of Physics, Stockholm university, Stockholm SE-10691, Sweden

 (Received 9 February 2022; revised 18 August 2022; accepted 8 September 2022; published 31 October 2022)

Measurements of any property of a microscopic system are bound to show significant deviations from the average, due to thermal fluctuations. For time-integrated currents such as heat, work, or entropy production in a steady state, it is in fact known that there will be long stretches of fluctuations both above as well as below the average, occurring equally likely at large times. In this paper we demonstrate that for any finite-time measurement in a nonequilibrium steady state—rather counterintuitively—fluctuations below the average are more probable. This discrepancy is found to be higher when the system is further away from equilibrium. For overdamped diffusive processes, there is even an optimal time when time-integrated current fluctuations mostly lie below the average. We demonstrate that these effects are consistent with a nonmonotonic skewness of current fluctuations and provide evidence that they are easily observable in experiments. We also discuss their extensions to discrete space Markov jump processes and implications to biological and synthetic microscopic engines.

DOI: [10.1103/PhysRevResearch.4.043067](https://doi.org/10.1103/PhysRevResearch.4.043067)

### I. INTRODUCTION

In microscopic nonequilibrium systems, individual measurements of heat, work, or entropy production can significantly fluctuate about the average values [1]. The nature of these fluctuations are constrained within the framework of stochastic thermodynamics by some universal results [2]. The most celebrated ones are the fluctuation theorems (see review [3] and references therein) which constrain the probability distributions of thermodynamic quantities such as heat, work, and entropy production. Its applications range from estimating free-energy differences in single molecule experiments [4,5] to determining the nature of efficiency fluctuations in microscopic engines [6–8]. Another class of results provide bounds on the fluctuations of *currents* in nonequilibrium steady states in terms of the steady-state entropy production rate  $\sigma = \langle \Delta S_{\text{tot}} \rangle / t$  [9]. For any current  $J$  in a stationary state of a continuous time, Markov process, it can be shown that the scaled cumulant generating function  $\phi_J^\sigma(\lambda, t) \equiv \frac{1}{t} \log \langle e^{-\lambda \sigma t} \frac{J}{\sigma} \rangle_t$  is bounded from below by a parabola [9–11],

$$\phi(\lambda, t) \geq -\sigma\lambda(1 - \lambda). \quad (1)$$

Terminating the expansion of  $\phi$  to the second order in  $\lambda$ , leads to the thermodynamic uncertainty relations [12–14] which are tradeoff relations connecting the precision of arbitrary current measurements to the entropy production rate.

In the  $t \rightarrow \infty$  limit, the left-hand side of Eq. (1) converges to a time-independent function [9] referred to as the large deviation rate function [15–19], knowing which helps fully characterize the fluctuations in the long-time limit. In general, such long-time results can be obtained within the mathematical framework of large deviation theory and many such results have been obtained for the statistics of the fluctuations of entropy production [20–25], efficiency distributions [6–8], first passage problems [26–28], and current fluctuations in general [29,30]. An interesting addition to this class of results was obtained in Ref. [31], where it was shown that the fraction of time that a current spends above its average value follows the arcsine law in the long time limit [32]. As a consequence, stochastic currents with long streaks above or below their average value are much more and equally likely than those that spend similar fractions of time above and below their average.

The other extreme of very short-time fluctuations of currents, is also surprisingly nontrivial. It has been shown that Eq. (1) saturates for  $J = \Delta S_{\text{tot}}$  in the limit  $t \rightarrow 0$  for overdamped diffusive processes [33–36]. As a consequence,  $\sigma$  can be exactly inferred for such systems by studying the mean and variance of current fluctuations at short times [33–36], even for nonstationary systems [37]. The saturation of the bound also implies that the fluctuations of  $\Delta S_{\text{tot}}$  are Gaussian in these systems in the short-time limit even when arbitrarily far from equilibrium [33]. In fact, as was recently pointed out, the Gaussianity in the  $t \rightarrow 0$  limit holds for any arbitrary current in overdamped diffusive processes [37]. As we show below, this short-time behavior combined with the large-deviation

\*sreekanth.km@fysik.su.se

†These authors contributed equally.

‡ayan@iiserkol.ac.in

§Electronic address: supriya@fysik.su.se

results mentioned above hold important clues for interesting finite-time fluctuation properties.

Finite-time fluctuations are clearly of interest since this is most often what is observed in experiments. However, when neither the  $t \rightarrow \infty$  nor the  $t \rightarrow 0$  limit can be taken, generic features of such fluctuations are harder to identify because of the prevalence of transient effects and time-correlations. If the  $t \rightarrow \infty$  limit can be thought in terms of applying a thermodynamic limit [38], then finite-time fluctuations include effects which vanish in the thermodynamic limit, making them harder to access. Some important general results in this category include the integral fluctuation theorem for stochastic entropy production [39], statistical properties of entropy production derivable from the fluctuation theorem [40], the finite-time versions of the thermodynamic uncertainty relations [11,41–43], universal results known for the statistics of infima, stopping times, and first-passage probabilities of entropy production [44], a generic equation describing the time evolution of the stochastic entropy production [45], statistics of the time of the maximum of a one dimensional stationary process [46], and bounds on first passage times of current fluctuations [47].

In this paper, we unravel a previously unnoticed property of current fluctuations at finite and short times. We demonstrate that the *skewness* of current fluctuations is positive and non-monotonic in time and argue that this behavior is generic for nonequilibrium steady states generated by any overdamped diffusive process. An expected consequence of this, which we find also holds true here is that at all finite times, current fluctuations below the long-time average are more probable than those above. For a single realization of the process, interestingly, this implies that a below average outcomes will be typical. Moreover, due to the nonmonotonicity, there is an optimal time when this discrepancy is the highest. We show that these features of current fluctuations are easily visible in nontrivial models studied numerically and experimentally and conjecture that they universally hold true. We also discuss their extensions to discrete space Markov jump processes and implications to biological and synthetic microscopic engines. In all cases, in the limit of large  $t$ , we recover results consistent with Ref. [31].

## II. RESULTS

The central results we present in this manuscript apply to nonequilibrium systems in a stationary state. We first consider generic overdamped diffusive processes of the form,

$$\dot{\mathbf{x}}(t) = \mathbf{A}[\mathbf{x}(t)] + \mathbf{B}[\mathbf{x}(t), t] \cdot \boldsymbol{\eta}(t), \quad (2)$$

where  $\mathbf{A}(\mathbf{x})$  is the drift vector, and  $\mathbf{B}(\mathbf{x}, t)$  is a  $d \times d$  matrix, and  $\boldsymbol{\eta}(t)$  represents a Gaussian white noise satisfying  $\langle \eta_i(t) \eta_j(t') \rangle = \delta_{ij} \delta(t - t')$ . Consider a current  $J$  in the stationary state of this system defined as  $J = \int_{\mathbf{x}(0)}^{\mathbf{x}(t)} \mathbf{d}(\mathbf{x}) \circ d\mathbf{x}$ , where  $\mathbf{d}(\mathbf{x})$  is any arbitrary function of  $\mathbf{x}$ , and  $\circ$  corresponds to the Stratanovich product. First we look at the implications of Eq. (1) for any such current. Without loss of generality, we consider currents for which  $\langle J \rangle \geq 0$ . Let  $\langle [J(t)]^k \rangle$  be the  $k$ th cumulant of  $J$  [48]. Expanding the inequality in Eq. (1) in powers of  $(-\lambda)^i$ , it can be shown that  $\langle [J(t)]^k \rangle \geq 0$  for  $k \geq 2$  for any  $t$ . For  $1 < k \leq 3$ , the cumulants coincide with the  $k$ th

central moment of  $J$ . Here  $\langle \cdot \rangle$  corresponds to an ensemble average over steady-state trajectories of length  $t$ . An important standardized moment which can then be constructed is the skewness,  $S = \frac{\langle [J(t)]^3 \rangle}{(\langle [J(t)]^2 \rangle)^{3/2}}$ . Skewness quantifies the asymmetries of the fluctuations about the average value. Here we focus on the properties of the skewness as a function of  $t$ . Using the results in Ref. [37] which proved the Gaussianity of general current fluctuations in the  $t \rightarrow 0$  limit (see Eqs. S13–S15 in Supplementary Note 1 of Ref. [37], where it is shown that  $\langle J(t) \rangle$  and  $\langle J(t)^2 \rangle$  are  $\propto t$  for small  $t$ , but  $\langle J(t)^3 \rangle \propto t^2$  for small  $t$ . For  $J = \Delta S_{\text{tot}}$ , this behavior was shown already in Ref. [33]), we obtain that  $S \propto t^{1/2}$  for small  $t$ . Further, the existence of the large deviation function  $\Phi(\lambda) = \lim_{t \rightarrow \infty} \phi(\lambda, t)$  ensures that all the cumulants scale linearly in time as  $t \rightarrow \infty$ . As a result,  $S \propto t^{-1/2}$  for large  $t$ . Combining these two limiting behaviours with the positivity of the cumulants, we obtain that  $S$  is a positive, nonmonotonic function of time that vanishes both in the  $t \rightarrow \infty$  limit as well as the  $t \rightarrow 0$  limit. As a consequence, there will also be a special time, where the skewness attains a maximum value. This is the first central observation we make in this paper.

From the generality of the above arguments, we expect this behavior to be generic for any nonequilibrium steady-state current if the short-time and long-time behavior are as detailed above. But to be more concrete, we now take the example of the nonequilibrium steady state of a colloidal system [24,36,49–52]. The model consists of a single colloidal particle in a harmonic trap with stiffness  $\kappa$ , whose mean position is modulated according to the Ornstein-Uhlenbeck process. The dynamics of the system with position variable  $x(t)$  and the trap center  $x_0(t) \equiv \lambda(t)$  can be described using a system of overdamped Langevin equations as

$$\begin{aligned} \dot{x}(t) &= -\frac{x(t) - \lambda(t)}{\tau} + \sqrt{2D}\zeta(t), \\ \dot{\lambda}(t) &= -\frac{\lambda(t)}{\tau_0} + \sqrt{2A}\xi(t). \end{aligned} \quad (3)$$

Here  $D$  is the diffusion constant at room temperature ( $T$ ),  $\tau = \gamma/\kappa$  is the relaxation time of the harmonic trap,  $\kappa$  is the trap stiffness, and  $\gamma$  is the drag coefficient related to  $D$  by the Stokes-Einstein relation as  $D\gamma = k_B T$ . Similarly,  $\tau_0$  is the relaxation time of the OU process and  $A$  corresponds to its strength. The noise terms  $\zeta(t)$  and  $\xi(t)$  are Gaussian white noises obeying  $\langle \xi(t) \rangle = 0$ ,  $\langle \zeta(t) \rangle = 0$ ,  $\langle \xi(t) \xi(t') \rangle = \delta(t - t')$ ,  $\langle \zeta(t) \zeta(t') \rangle = \delta(t - t')$ , and  $\langle \xi(t) \zeta(t') \rangle = 0$ .

In Fig. 1, we plot the skewness  $S$  of several arbitrary currents as a function of time, using numerical data. Currents are constructed using  $J = \int_{\mathbf{x}(0)}^{\mathbf{x}(t)} \mathbf{d}(\mathbf{x}) \circ d\mathbf{x}$ , where  $\mathbf{x} = [x; \lambda]^T$  and  $\mathbf{d}(\mathbf{x}) = [c_1 x + c_2 \lambda; c_3 x + c_4 \lambda]^T$ . Here  $\{c_i\} \in \mathbb{R}$  are constants which can be varied to construct different currents. Without loss of generality, we consider currents with  $\langle J \rangle \geq 0$ . We find that the skewness of arbitrary currents is a positive, bounded, and nonmonotonic function of  $t$  which vanishes both in the short-time limit as  $t^{1/2}$  and in the large-time limit as  $t^{-1/2}$ . Next, we investigate these properties for a particular choice of the current, which is  $J = \Delta S_{\text{tot}}$  [53]. The corresponding entropy production rate is given by  $\sigma = \frac{\delta^2 \theta}{(\delta+1)\tau_0}$ , where  $\delta = \frac{\tau_0}{\tau}$  and  $\theta = \frac{A}{D}$  [24,50,52]. In Fig. 2(a), we plot the analytically

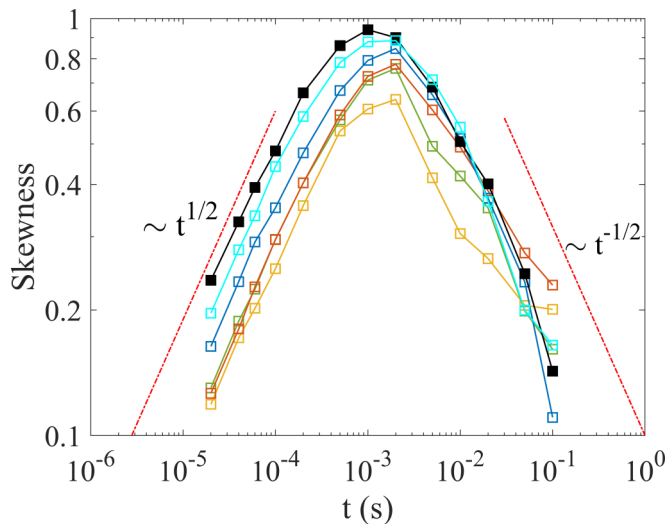


FIG. 1. The skewness  $S$  of arbitrary currents (shown in colors) in nonequilibrium steady state of the stochastic sliding parabola model as a function of  $t$ . The vanishing of  $S(t)$  in the  $t \rightarrow 0$  limits shows the emergence of Gaussian fluctuations in the short-time limit. The solid black line corresponds to  $J = \Delta S_{\text{tot}}$ . The red dashed lines corresponds to power-law fits at the short and large  $t$  limits.

computed skewness of  $\Delta S_{\text{tot}}(t)$ , for different values of  $\theta$  [54]. As expected, we find that  $S(t) \geq 0$  and is nonmonotonic in time, featuring a maximum at an intermediate time  $t \equiv \tau_E$ . We also find that the skewness increases with  $\theta$ , which also increases the entropy production rate of the system.

Now we look at the measurable consequences of this nonmonotonicity. We first consider the mean fraction of the time when the measured entropy stays above the average value,

denoted by  $\langle T_+ \rangle = \frac{1}{t} \int_0^t \Theta[J(s) - \langle J(s) \rangle] ds$ , where  $\Theta(x)$  is the Heaviside function. If the fluctuations of  $\Delta S_{\text{tot}}(t)$  were symmetric about the average, then it would have implied,  $\langle T_+ \rangle = \frac{1}{2}$ . Indeed, this is known to be the case in the  $t \rightarrow \infty$  limit [31]. In Fig. 2(b), we plot  $\langle T_+ \rangle$ , obtained from the numerical data as a function of  $t$ . We find that  $\langle T_+ \rangle < \frac{1}{2}$  for all  $t$  and tends to  $\frac{1}{2}$  in the limits  $t \rightarrow 0$  and  $t \rightarrow \infty$ . We also find that  $\langle T_+ \rangle$  is nonmonotonic in time and attains a minimum close to when  $S(t)$  is the highest.

Interestingly, the behavior of  $\langle T_+ \rangle$  implies that it is more likely that a current measured for a finite  $t$  duration stays below the average value for most part of the measurement. This discrepancy is the highest when the skewness peaks. We also find that  $\langle T_+ \rangle$  is monotonically decreasing as a function of  $\theta$  for all  $t$ . Hence, the further away the system is from equilibrium, the more likely that arbitrary currents or entropy production measured along a single trajectory stay below the average value for most of the time.

Next we consider  $\langle T_{\text{max}}(t) \rangle$ , where  $T_{\text{max}}(t) = \frac{t_{\text{sup}}}{t}$ , where  $t_{\text{sup}}$  is the time of global maximum of  $\Delta S_{\text{tot}}(t) - \sigma t$ . The results are shown in Fig. 2(c). We find that  $\langle T_{\text{max}} \rangle$  has a similar time dependence as  $\langle T_+ \rangle$  and stays below  $\frac{1}{2}$  for all  $t$  and tends to  $\frac{1}{2}$  in the limits  $t \rightarrow 0$  and  $t \rightarrow \infty$ .  $\langle T_{\text{max}}(t) \rangle$  is also found to be nonmonotonic in time featuring a minimum at  $t \sim \tau_E$ . This means, for currents measured for a finite time, it is more likely that its maximum deviation above the mean will be found before the half-length of the measurement. Again, the discrepancy will be the highest when  $t \sim \tau_E$ .

As seen in Fig. 1, the time at which the skewness has the highest value varies from current to current. In particular, for  $J = \Delta S_{\text{tot}}$ , from the analytical solutions, we find that  $\tau_E$  monotonically decreases with increasing  $\theta$  (see Appendix A where the dependence of  $\tau_E$  on  $\theta$  and  $\tau_0$  is analytically ob-

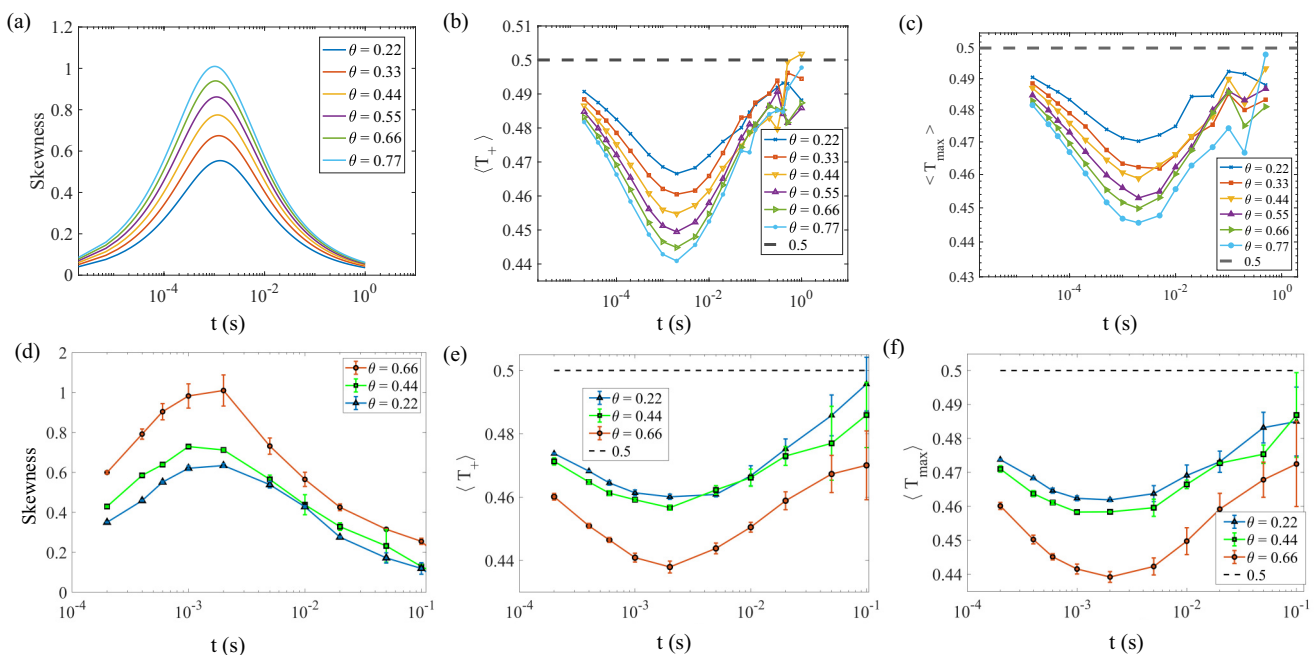


FIG. 2. (a) Skewness of  $\Delta S_{\text{tot}}$  as a function of  $t$  computed analytically for the model in Eq. (2). (b)  $\langle T_+ \rangle$  and (c)  $\langle T_{\text{max}} \rangle$  as a function of  $t$  for different values of  $\theta$ , obtained from numerical simulation of the system. In panels (d)–(f), we show the same results obtained from the experimental realization of the same system.

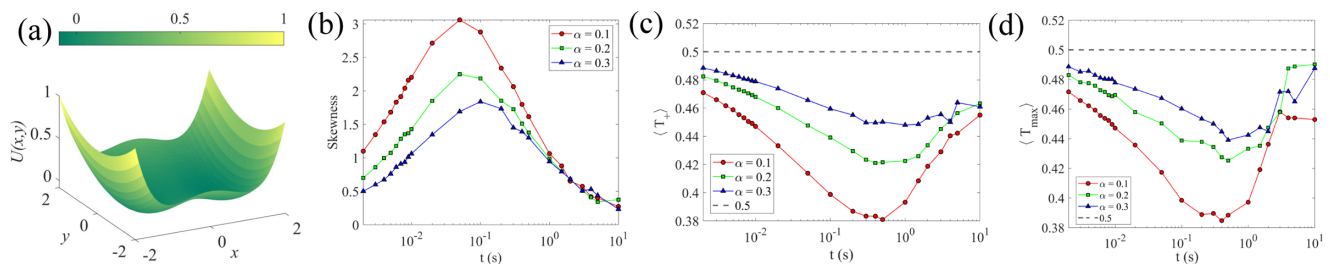


FIG. 3. (a) Double-well potential with  $b = 1$  and  $k = 2$  (see the details in Ref. [57]). (b) Skewness, (c)  $\langle T_+ \rangle$ , and (d)  $\langle T_{\max} \rangle$  of the entropy currents as a function of  $t$ , obtained numerically for the gyrator model with double-well confining potential for different values of the ratio of the temperatures ( $\alpha = T_2/T_1$ ) along the two orthogonal directions of the gyrator system. See Appendix B for relevant details of the model.

tained). As a result, in order to capture the non monotonic nature of  $S(t)$ , the further a system is away from equilibrium, the finer the resolution needs to be. We demonstrate below that this is, however, still very detectable in experimental data.

*Experiments.* The model in Eq. (3) was first realized in an optical tweezers setup in Ref. [49] and was also studied recently in Ref. [36]. To realize this system, we trap a  $3 \mu\text{m}$  polystyrene particle in an aqueous solution in a harmonic potential well given by  $U[x(t), \lambda(t)] = k[x(t) - \lambda(t)]^2/2$ , where the trap stiffness is  $k = 19.7 \pm 0.1 \text{ pN}/\mu\text{m}$ . Here  $\lambda(t)$  is the time-dependent mean position of the trap which is modulated using an acousto-optic modulator according to an Ornstein-Uhlenbeck process [see Eq. (3)] with  $\tau_0 = 2.5 \text{ ms}$ , and  $A = [0.1, 0.2, 0.3] \times (0.6 \times 10^{-6})^2 \text{ m}^2/\text{s}$ . We sample the one-directional trajectory of the probe at a spatiotemporal resolution of  $\sim 1 \text{ nm}-10 \text{ kHz}$  for 100 s. We then use the autocorrelation of the time series of a trapped particle and the noise to calibrate the fluctuation of the probe from volts to nanometers [55]. We plot the experimental results in Figs. 2(d), 2(e) and 2(f). We find that the numerical results in Figs. 2(a)–2(c) are reproduced by our experiments and that the nonmonotonies in  $S(t)$ ,  $\langle T_+ \rangle$ , and  $\langle T_{\max} \rangle$  are clearly visible [56]. So far, we have considered a linear Langevin model. However, as we argued, the nonmonotonic nature of skewness is expected to hold for any overdamped diffusive process. To substantiate this, we numerically study fluctuations of entropy currents of a system with nonlinearities. For this, we consider an anharmonic Brownian gyrator with a double-well confining potential (studied recently in Ref. [57]; see Appendix B for details and for the additional example of a gyrator with a quartic confining potential). We vary the nonequilibrium conditions by changing the ratio of the temperatures ( $\alpha = T_2/T_1$ )

along the two orthogonal directions. In Fig. 3, we show that all the features that we showed in Fig. 2 are also present in this nonlinear model.

Apart from the generic bound in Eq. (1) which holds for any continuous-time Markov process, a crucial ingredient in our results is the emergence of Gaussian fluctuations in the short-time limit of overdamped diffusive systems, recently proved in Ref. [37]. For discrete-space systems, which evolve according to a continuous-time Markov process, current fluctuations are not necessarily Gaussian at  $t \rightarrow 0$ ; in fact, it can be shown that all the moments scale  $\propto t$  at short times (see the details in Appendix C). Thus, the skewness will scale  $\propto t^{-1/2}$ , diverging as  $t \rightarrow 0$ , and will not necessarily be nonmonotonic in time. We see again that shorter current measurements in such systems are more likely to lie below the average. In all the cases these effects increase when the system is further away from equilibrium. In Fig. 4, we demonstrate this for a three-level system, coupled to two thermal reservoirs at unequal temperatures [58–60]. Variants of this system have recently appeared in a number of different contexts [61–63], an important example being classical/quantum clocks [64]. It is known that clocks need to run for a long time to give reliable estimates [65] which is also the limit in which the skewness vanishes.

### III. CONCLUSIONS

In summary, we have unravelled and quantitatively characterized the universal properties of finite-time skewness of current fluctuations, and their measurable consequences in nonequilibrium steady states. For overdamped diffusive systems, we have demonstrated that the skewness of currents must be positive and nonmonotonic in time, vanishing in

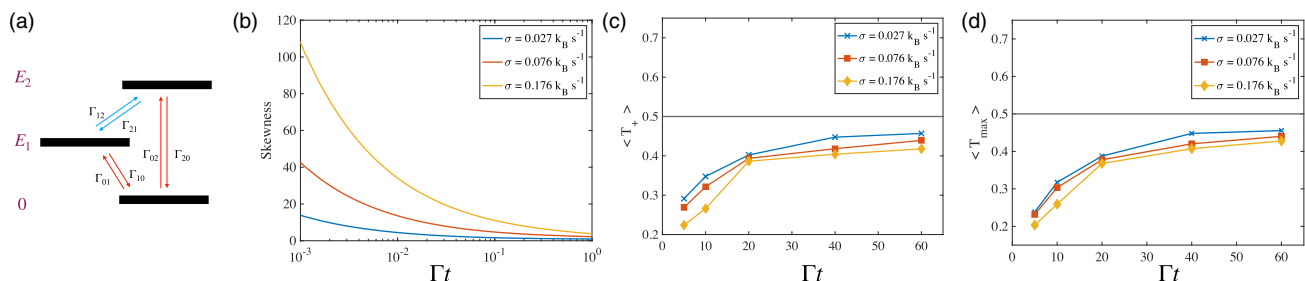


FIG. 4. (a) Three-level system. (b) Skewness of  $\Delta S_{\text{tot}}$ , (c)  $\langle T_+ \rangle$ , and (d)  $\langle T_{\max} \rangle$  as a function of  $t$  computed analytically for the three-level system. See Appendix C for details and the choice of the parameters.

the  $t \rightarrow 0, t \rightarrow \infty$  limits. It is also found to peak at an experimentally accessible, short-time which varies with the system parameters. For discrete space systems evolving according to a continuous time Markov jump processes, we show that skewness is not necessarily nonmonotonic, and diverges to  $+\infty$  in the  $t \rightarrow 0$  limit. The results imply that, rather counter intuitively, it is more probable that currents such as entropy production will mostly lie below average in a single realization of finite-time duration. For overdamped diffusive processes, we find there is even an optimal time when this discrepancy is the highest.

Although we provide numerical and experimental evidence, we remark that we have not proved the positivity of  $1/2 - \langle T_+(t) \rangle, 1/2 - \langle T_{\max}(t) \rangle$  and their nonmonotonicity in a generic setting. We have shown the positivity of skewness for overdamped diffusive processes and Markov jump processes and its nonmonotonicity in time in the former case. However, that alone does not always imply the observed properties of current fluctuations; for example, it is known that there exist probability distributions with positive skewness where nevertheless the mean is less than the mode [66]. Based on the extensive evidence at hand, however, it is a reasonable conjecture that the probability distribution of time integrated currents in nonequilibrium systems is so constrained that the results we find here generically hold.

Our results can be potentially verified in molecular motors such as kinesin [67] by looking at the statistics of its steps [68] or energy dissipation [69]. Our results also show that the nature of the fluctuations of currents, and thus the most probable outcome, crucially depend on the time duration of the measurement. It would be of substantial interest to investigate whether biological motors have optimized their timescales considering such constraints (through molecular evolution). For artificial microscopic engines such as the ones studied in Refs. [70–75], this implies that it might be possible to choose cycling times to optimize fluctuations, and to get a reliable performance in a limited number of runs. We plan to attempt answering these questions in our future research.

**Data and Code Availability** The raw data files and codes are available openly at Ref. [81].

**ACKNOWLEDGMENTS**

Nordita is partially supported by Nordforsk. S.K. acknowledges the support of the Swedish Research Council (Vetenskapsrådet) through the Grant No. 2021-05070. B.D. is thankful to Ministry of Education of Government of India for the financial support through the Prime Minister’s Research Fellowship (PMRF) grant. A.K. acknowledges the DST, Government of India for INSPIRE Fellowship.

**APPENDIX A: EXACT CALCULATION OF THE MGF OF  $\Delta S_{\text{tot}}(t)$  FOR THE STOCHASTIC SLIDING PARABOLA (SSP) MODEL**

In this section, we reproduce the exact calculation of the moment generating function of  $\Delta S_{\text{tot}}(t)$  for the Stochastic Sliding Parabola model, previously obtained in Ref. [52]. The stationary probability distribution for  $x$  and  $\lambda$  is given by [50]

$$p_{\text{st}}[x(t), \lambda(t)] = \frac{\exp \left\{ -\frac{(\delta+1)[\delta^2\theta(x-\lambda)^2 + \delta(\theta x^2 + \lambda^2) + \lambda^2]}{2D\tau_0\theta[\delta^2(\theta+1)+2\delta+1]} \right\}}{2\pi\sqrt{\frac{D^2\tau_0^2\theta[\delta^2(\theta+1)+2\delta+1]}{\delta(\delta+1)^2}}}, \quad (\text{A1})$$

the MGF of total entropy production  $\Delta S_{\text{tot}}(t)$  can be written down in the following manner. First, the joint probability density functional of trajectories starting at  $t = 0$  at  $(x_0, \lambda_0)$  and ending at  $t = \tau$  at  $(x_t, \lambda_t)$  may be written as

$$P[x(\cdot), \lambda(\cdot)] = N \exp \left\{ -\int_0^t ds L(\dot{x}(s), x(s), \dot{\lambda}(s), \lambda(s), s) \right\}, \quad (\text{A2})$$

with the Lagrangian

$$L = \frac{1}{4D} \left( \left[ \dot{x} + \frac{\delta(x-\lambda)}{\tau_0} \right]^2 + \frac{1}{\theta} \left[ \dot{\lambda} + \frac{\lambda}{\tau_0} \right]^2 \right). \quad (\text{A3})$$

The normalization constant  $N$  for this case is [78],

$$N = \exp \left( \frac{1}{2} \left[ \frac{\delta+1}{\tau_0} \right] t \right). \quad (\text{A4})$$

The entropy production in the steady state in the time interval  $[0, \tau]$  for the SSP is then

$$\Delta S_{\text{tot}}(t) = \frac{\delta}{D\tau_0} \int_0^t ds \lambda(s) \dot{x}(s) + \frac{\delta^2 \{ \delta[\theta(x_0^2 - x_t^2) + 2x_0\lambda_0 - 2x_t\lambda_t - \lambda_0^2 + \lambda_t^2] 2x_0\lambda_0 - 2x_t\lambda_t \}}{2D\tau_0[\delta^2(\theta+1)+2\delta+1]}. \quad (\text{A5})$$

This form of the entropy production can easily be obtained by equating it to the ratio of the probabilities of forward and time-reversed trajectories using Eqs. (A1) and (A2) and the form of the Lagrangian Eq. (A3). Hence, up to a normalization factor  $\mathbf{C}$  [determined by Eqs. (A1) and (A4)], we have the following expression for the MGF of  $\Delta S_{\text{tot}}(t)$ :

$$\langle e^{-\frac{u}{2} \Delta S_{\text{tot}}(t)} \rangle = \mathbf{C} \int dx_0 \int d\lambda_0 \int dx_t \int d\lambda_t \int_{x_0, \lambda_0}^{x_t, \lambda_t} \mathcal{D}[x(\cdot), \lambda(\cdot)] e^{-\beta S[x(\cdot), \lambda(\cdot), u]}, \quad (\text{A6})$$

with the augmented action

$$S[x(\cdot), \lambda(\cdot), u] = \frac{(\delta+1)[\delta^2\theta(x_0 - \lambda_0)^2 + \delta(\theta x_0^2 + \lambda_0^2) + \lambda_0^2]}{2D\tau_0\theta[\delta^2(\theta+1)+2\delta+1]} + \int_0^t ds \frac{1}{4D} \left\{ \left[ \dot{x} + \frac{\delta(x-\lambda)}{\tau_0} \right]^2 + \frac{1}{\theta} \left[ \dot{\lambda} + \frac{\lambda}{\tau_0} \right]^2 \right\} + \frac{u}{2} \Delta S_{\text{tot}}(t)[x, \lambda]. \quad (\text{A7})$$

After several partial integrations, it can be shown that the above quadratic action reduces to

$$S[x(\cdot), \lambda(\cdot), u] = \frac{1}{4D} [x \quad \lambda] \mathbf{A}_u \begin{bmatrix} x \\ \lambda \end{bmatrix} + \text{Boundary terms in } (x, \lambda, u), \tag{A8}$$

where the kernel is defined by the operator:

$$\mathbf{A}_u = \begin{bmatrix} -\frac{d^2}{ds^2} + \frac{\delta^2}{\tau_0^2} & k \frac{\delta}{\tau_0} \frac{d}{ds} - \frac{\delta^2}{\tau_0^2} \\ -k \frac{\delta}{\tau_0} \frac{d}{ds} - \frac{\delta^2}{\tau_0^2} & -\frac{1}{\theta} \frac{d^2}{ds^2} + \frac{1}{\theta\tau_0^2} + \frac{\delta^2}{\tau_0^2} \end{bmatrix}, \quad k \equiv 1 - u. \tag{A9}$$

Carrying out the Gaussian integral, and requiring the boundary terms to vanish, the generating function at arbitrary times  $\tau$  can be written down as a ratio of functional determinants,

$$\langle e^{-\frac{u}{2} \Delta S_{\text{tot}}(\tau)} \rangle = \sqrt{\frac{\det \mathbf{A}_{u=0}}{\det \mathbf{A}_u}} \equiv \Phi(u). \tag{A10}$$

This ratio can be computed using a technique described in Ref. [79] and used in Ref. [51], which is based on the spectral- $\zeta$  functions of Sturm-Liouville type operators. Applying this method, it can be shown that this ratio can be obtained in terms of a characteristic polynomial function  $F$  as

$$\begin{aligned} \langle e^{-\frac{u}{2} \Delta S_{\text{tot}}(\tau)} \rangle &= \sqrt{\frac{F(1)}{F(k)}}, \quad F(k) \\ &\equiv \text{Det}[M + NH(t)], \quad k = 1 - u, \end{aligned} \tag{A11}$$

where  $H$  is the matrix of suitably normalized fundamental solutions of the homogeneous equation,  $\mathbf{A}_u \vec{x} = 0$ , and is defined as

$$H(t) = \begin{bmatrix} x_1(t) & x_2(t) & x_3(t) & x_4(t) \\ \lambda_1(t) & \lambda_2(t) & \lambda_3(t) & \lambda_4(t) \\ \dot{x}_1(t) & \dot{x}_2(t) & \dot{x}_3(t) & \dot{x}_4(t) \\ \dot{\lambda}_1(t) & \dot{\lambda}_2(t) & \dot{\lambda}_3(t) & \dot{\lambda}_4(t) \end{bmatrix}, \quad H(0) = \mathbf{I}_4. \tag{A12}$$

$M$  and  $N$  have information about the boundary conditions from Eq. (A8) and we require

$$M \begin{bmatrix} \vec{x}(0) \\ \dot{\vec{x}}(0) \end{bmatrix} = 0, \quad N \begin{bmatrix} \vec{x}(t) \\ \dot{\vec{x}}(t) \end{bmatrix} = 0. \tag{A13}$$

A derivation of Eq. (A11), applicable to a class of driven Langevin systems with quadratic actions is given in Ref. [51]. We also stress that the expression given in Eq. (A11) is valid only for  $u \in [u^-(\tau), u^+(\tau)]$  for which the operator  $A_u$  does not have negative eigenvalues. The MGF is not analytic outside this interval.

For the SSP in the steady state, we find the four independent solutions of  $A_u \vec{x} = 0$  to be

$$\vec{x}_i = \begin{bmatrix} x_i(t) \\ \lambda_i(t) \end{bmatrix}, \quad i = 1 \text{ to } 4, \tag{A14}$$

where

$$\lambda_i(t) = 1 \exp \left( \pm \frac{\tau \sqrt{\frac{\delta^2 \theta + \delta^2 + \delta^2 \theta [-(1-u)^2] \pm \tau_0^2 \sqrt{\frac{\delta^4 [\theta - \theta(1-u)^2 + 1]^2 - 2\delta^2 \{ \theta(1-u)^2 - 1 \} + 1}}{\tau_0^4}}}{\sqrt{2}}}{\tau_0^2} \right), \tag{A15}$$

$$x_i(t) = 1 \frac{\tau_0 \{ (u-1) \lambda_i'(t) [\delta^2 \theta (u-2)u - 1] + \tau_0 [\delta \lambda_i''(t) + \tau_0 (u-1) \lambda_i^{(3)}(t)] \} + \delta \lambda_i(t) [\delta^2 \theta (u-2)u - 1]}{\delta^3 \theta (u-2)u}. \tag{A16}$$

Matrices  $M$  and  $N$  are given by

$$M = 1 \begin{pmatrix} \frac{[1-(1-u)\theta]\delta^3 + 2\delta^2 + \delta}{2D[(\theta+1)\delta^2 + 2\delta + 1]\tau_0} & \frac{\delta\{[(1-u)\theta - 1]\delta^2 - u\delta - u + 1\}}{2D[(\theta+1)\delta^2 + 2\delta + 1]\tau_0} & -\frac{1}{2D} & 0 \\ -\frac{(2-u)\delta^2(\delta+1)}{2D[(\theta+1)\delta^2 + 2\delta + 1]\tau_0} & \frac{(2-u)\theta\delta^3 + (\theta+1)\delta^2 + 2\delta + 1}{2D\theta[(\theta+1)\delta^2 + 2\delta + 1]\tau_0} & 0 & -\frac{1}{2D\theta} \\ 0 & 0 & 0 & 0 \\ 0 & 0 & 0 & 0 \end{pmatrix}, \tag{A17}$$

$$N = 1 \begin{pmatrix} 0 & 0 & 0 & 0 \\ 0 & 0 & 0 & 0 \\ \frac{\delta\{[(1-u)\theta + 1]\delta^2 + 2\delta + 1\}}{2D[(\theta+1)\delta^2 + 2\delta + 1]\tau_0} & -\frac{\delta[(1-u)\theta\delta^2 + \delta^2 + (1-u)\delta - u + 1]}{2D[(\theta+1)\delta^2 + 2\delta + 1]\tau_0} & \frac{1}{2D} & 0 \\ -\frac{u\delta^2(\delta+1)}{2D[(\theta+1)\delta^2 + 2\delta + 1]\tau_0} & \frac{(\theta - (1-u)\theta)\delta^3 + (\theta+1)\delta^2 + 2\delta + 1}{2D\theta[(\theta+1)\delta^2 + 2\delta + 1]\tau_0} & 0 & \frac{1}{2D\theta} \end{pmatrix}. \tag{A18}$$

Using these, the MGF can be computed exactly using Eq. (A11), and various moments of the probability distribution can also be exactly obtained for any  $t$ .

**Dependence of  $\tau_E$  on system parameters**

For the stochastic sliding parabola model, it is possible to analytically compute how  $\tau_E$ , the time at which Skewness

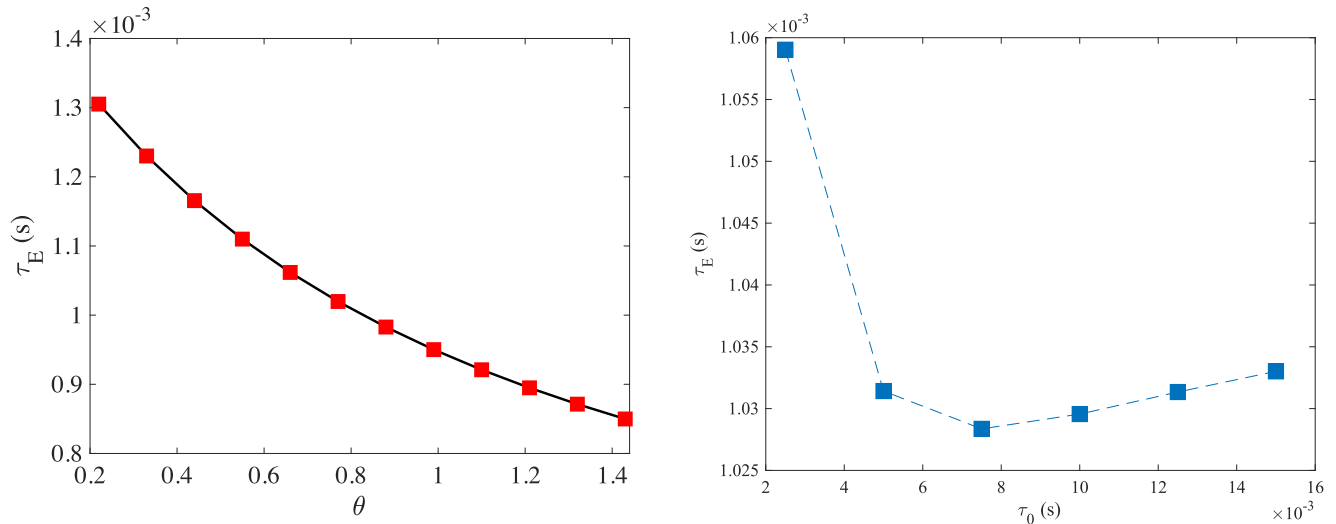


FIG. 5. (a) Dependence of  $\tau_E$  on the relative magnitude of the Ornstein Uhlenbeck driving  $\theta$ . We find that  $\tau_E$  monotonically decreases with increasing  $\theta$ , which is the limit at which the system goes further away from equilibrium. (b) Dependence of  $t_E$  on  $\tau_0$ . We find that  $\tau_E$  is a nonmonotonic function of  $\tau_0$  and features a minimum at a particular  $\tau_0$  value.

peaks, depends on the system parameters, using the exact expressions. In Fig. 5, we demonstrate how  $\tau_E$  depends on  $\theta$  and  $\tau_0$ . We find that  $\tau_E$  monotonically decreases with increasing  $\theta$ , which is the limit at which the system goes further away from equilibrium. This means, further away the system is from equilibrium, a higher resolution in time will be required to see the nonmonotonicity in current fluctuations. The dependence of  $\tau_E$  on  $\tau_0$  is found to be more nontrivial. We find that  $\tau_E$  is a nonmonotonic function of  $\tau_0$  and features a minimum at a particular  $\tau_0$  value.

**APPENDIX B: ENTROPY CURRENTS OF ANHARMONIC BROWNIAN GYRATORS**

The Brownian gyrotor is one of the minimal prototypes of a microscopic heat engine [72,73,75]. It consists of a micron-sized particle trapped in a generic potential well, coupled to two heat reservoirs with different temperatures along two orthogonal directions. When the two degrees of freedom of the trapped particle are coupled, it can be shown that the system reaches a nonequilibrium stationary state, where the particle starts gyrating around the minima of the potential. The dynamics of the system, in the overdamped limit, can be expressed in terms of coupled Langevin equations:

$$\gamma \dot{x} = -\frac{\partial U(x, y)}{\partial x} + \sqrt{2\gamma k_B T_1} \eta_1(t), \tag{B1}$$

$$\gamma \dot{y} = -\frac{\partial U(x, y)}{\partial y} + \sqrt{2\gamma k_B T_2} \eta_2(t). \tag{B2}$$

Here,  $U(x, y)$  denotes the confining potential in the  $x$ - $y$  plane. The  $x$  axis is coupled to a thermal reservoir at temperature  $T_1$  and the  $y$  axis is coupled to another thermal reservoir at temperature  $T_2$ . The corresponding thermal noises  $\eta_i(t)$  are of Gaussian nature and white in time, such that  $\langle \eta_i(t) \rangle = 0$  and  $\langle \eta_i(t) \eta_j(t') \rangle = \delta_{ij} \delta(t - t')$ . The viscous drag of the medium is denoted by  $\gamma$ , which is related to the temperatures of the reservoirs through the Einstein relation,  $D_i \gamma = k_B T_i$ ,  $k_B$  is the Boltzmann constant (we set  $k_B = 1$  for simplicity). In this

work, we choose the anharmonic Brownian gyrotor, where the confining potential is anharmonic [57,74], as an example of a nonlinear diffusive model.

We first consider a Brownian gyrotor with a double-well confining potential of the form

$$U_{dw}(x', y') = x'^4 - 2bx'^2 + \frac{1}{2}ky'^2, \tag{B3}$$

where axes of the potential  $x'$  and  $y'$  are rotated by an angle  $\theta$  with respect to the temperature axes  $(x, y)$  (axes of the coordinate frame) as

$$\begin{bmatrix} x' \\ y' \end{bmatrix} = \begin{bmatrix} \cos \theta & -\sin \theta \\ \sin \theta & \cos \theta \end{bmatrix} \times \begin{bmatrix} x \\ y \end{bmatrix}. \tag{B4}$$

The parameter “ $b$ ” can be used to tune the bi-stable nature of the potential along the  $x'$  direction as the barrier height ( $= b^2$ ) and the position of the minima ( $= \pm \sqrt{b}$ ) of the potential are dependent on it. The stiffness constant “ $k$ ” characterizes the harmonic part of the potential along the  $y'$  direction. We choose  $b = 1$ ,  $k = 2$ , and  $\theta = 45^\circ$  for the analysis performed in this work.

We also consider another anharmonic Brownian gyrotor with a quartic confining potential given by

$$U_{qw}(x', y') = (k_1 x'^2 + k_2 y'^2)^2. \tag{B5}$$

The parameters “ $k_1$ ” and “ $k_2$ ” can be considered as the stiffness constants along the respective directions. We set  $k_1 = 1$ ,  $k_2 = 2$  along with  $\theta = 45^\circ$  to construct an anisotropic quartic potential for the analysis performed in this work.

The entropy currents for both gyrotors are constructed numerically with third-order polynomial basis functions using the TUR-based short-time inference scheme [33–35], as described in Refs. [57,80]. We have looked into the properties of entropy currents corresponding to the different nonequilibrium conditions controlled by the ratios of the temperatures ( $\alpha = T_2/T_1$ ) of the thermal reservoirs of the systems, where  $\alpha = 0.1$  corresponds to the most nonequilibrium configuration we considered, and  $\alpha = 0.3$  is the least nonequilibrium configuration of both systems. The nonmonotonic features of

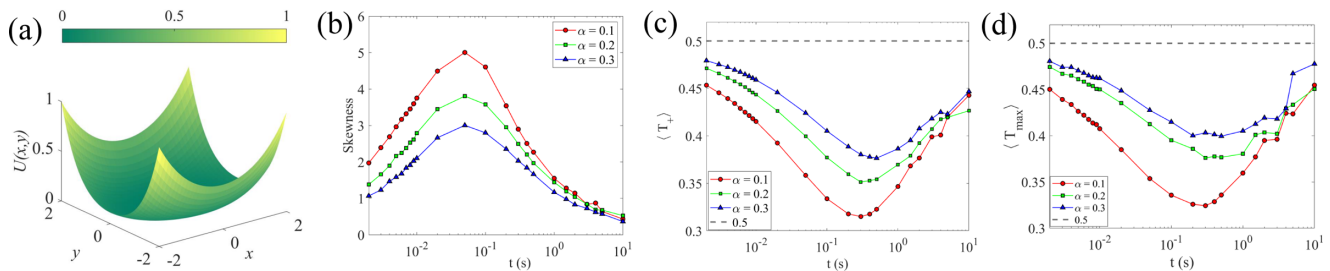


FIG. 6. (a) Quartic confining potential with “ $k_1$ ” = 1 and “ $k_2$ ” = 2. (b) Skewness, (c)  $\langle T_+ \rangle$ , and (d)  $\langle T_{\max} \rangle$  of the entropy currents as a function of  $t$ , obtained numerically for the gyrator model with a quartic confining potential for different values of the ratio of the temperatures ( $\alpha = \frac{T_2}{T_1}$ ).

the entropy current fluctuations for the gyrator system with double-well confining potential are shown in Fig. 3 of the main text and in Fig. 6 we show the similar results for the quartic well confining potential.

### APPENDIX C: SKEWNESS OF CURRENTS IN CONTINUOUS-TIME MARKOV JUMP PROCESSES

Here we demonstrate that Skewness  $\propto t^{-1/2}$  in the  $t \rightarrow 0$  limit for discrete space system evolving according to a continuous time Markov jump process. We consider a set of  $M$  number of states  $\{i\}$ ,  $i = 1, 2, \dots, M$ , and transition rates  $\Gamma_{ij} \geq 0$ . Let  $\pi(i)$  correspond to the steady-state probability of finding the system in the state  $i$ . A stochastic realization of the system is denoted by  $x(s) \in \{i\}$  with  $s \in [0, t]$ . The fluctuating current between any two pairs of states  $i$  and  $j$  can be computed as

$$j_{ij}(t) = \sum_k \delta(s - s_k) [\delta_{x(s_k^+), j} \delta_{x(s_k^-), i} - \delta_{x(s_k^+), i} \delta_{x(s_k^-), j}], \quad (C1)$$

where  $x(s_k^+)$  [ $x(s_k^-)$ ] corresponds to the state of the system immediately after (before) the transition at times  $s = s_k$ . A generalized time-integrated current in this system is given by

$$J(t) = \int_0^t ds \sum_{i < j} d_{ij} j_{ij}(s), \quad (C2)$$

where  $d_{ij} = -d_{ji}$  are weighting factors which are constants. The steady-state average of this current is given by

$$\langle J(t) \rangle = t \sum_{ij} \pi(i) \Gamma_{ij} d_{ij}. \quad (C3)$$

A particular choice,  $d_{ij} = F_{ij} = \log \frac{\Gamma_{ij} \pi(i)}{\Gamma_{ji} \pi(j)}$ , corresponds to the current  $J = \Delta S_{\text{tot}}(t)$ .

The fluctuations of any such current  $J$  can be calculated using its moment generating function,

$$G(\lambda, t) = \langle e^{-\lambda J(t)} \rangle = \langle 1 | e^{t \mathcal{L}(\lambda)} | \pi \rangle, \quad (C4)$$

where  $\mathcal{L}(\lambda)$  is the tilted transition matrix with elements,

$$\mathcal{L}_{ij}(\lambda) = \Gamma_{ji} \exp(\lambda d_{ji}) - \delta_{ij} \sum_l \Gamma_{il}. \quad (C5)$$

We are particularly interested in the small time properties of the moments of the current  $J(t)$ . This can be obtained by Taylor expanding  $G$  as near  $t = 0$ . Keeping to first order in  $t$ , we obtain

$$G(\lambda, t) \sim 1 - t \langle 1 | \mathcal{L}_{ij}(\lambda) | \pi \rangle + \mathcal{O}[t^2]. \quad (C6)$$

For a generic choice of  $\Gamma_{ij}$  and  $d_{ij}$ , it is possible to verify that all the moments of  $J$ , obtained by Taylor expanding  $G$  as a function of  $\lambda$ , will be proportional to  $t$  for small  $t$ . Thus, the skewness as defined in the main text, will be proportional to  $t^{-1/2}$  for  $t \rightarrow 0$ .

In Fig. 4(a) of the main text, we show this for a three-level system  $x \in \{0, 1, 2\}$ , with energy levels  $E_i = \{0, E_1, E_2\}$ . We have assumed that the transitions between the levels 0 and 1, and the levels 0 and 2 are mediated by a hot reservoir at inverse temperature  $\beta_1 = \frac{1}{k_B T_1}$ , where  $k_B$  is the Boltzmann constant and  $T_1$  is the temperature of the hot reservoir. The corresponding transition rates obey the local detailed balance condition:

$$\Gamma_{01} = \exp(-\beta_1 E_1) \Gamma_{10}, \quad \Gamma_{02} = \exp(-\beta_1 E_2) \Gamma_{20}. \quad (C7)$$

The transitions between levels 1 and 2 are assumed to be mediated by a cold reservoir at inverse temperature  $\beta_2 = \frac{1}{k_B T_2} > \beta_1$ . The corresponding transition rates obey

$$\Gamma_{12} = \exp[-\beta_2 (E_2 - E_1)] \Gamma_{21}. \quad (C8)$$

The skewness of arbitrary currents and in particular entropy production can be straightforwardly computed for this model using the expressions given above. There are also standard techniques available to numerically simulate this model as a continuous time Markov process [82] and to obtain the statistics of fluctuating currents as a function of time. The plots in Fig. 4 of main text are obtained for the parameter choices  $E_1 = k_B T_1$ ,  $E_2 = 2k_B T_1$ ,  $\Gamma_{01} = \Gamma_{02} = \Gamma_{12} = 1s^{-1}$ ,  $\beta_1 = (k_B T_1)^{-1}$  and  $T_2 = T_1/2$ ,  $T_1/3$ , and  $T_1/5$ , for which the entropy production rates are,  $\sigma = 0.027k_B s^{-1}$ ,  $0.076k_B s^{-1}$ , and  $0.176k_B s^{-1}$ , respectively.

### APPENDIX D: PARAMETER VALUES

(1) Figure 1:  $\tau \equiv \frac{1}{2\pi f_c} = 0.0013$  s,  $\tau_0 = 0.0025$  s,  $D = 1.6452 \times 10^{-13}$  m<sup>2</sup>/s,  $A = 0.3 \times (0.6 \times 10^{-6})^2$  m<sup>2</sup>/s.

(2) Figure 2: (a–c)  $\tau \equiv \frac{1}{2\pi f_c} = 0.0013$  s,  $\tau_0 = 0.0025$  s,  $D = 1.6452 \times 10^{-13}$  m<sup>2</sup>/s,  $A = [0.1, 0.15, 0.2, 0.25, 0.3, 0.35] \times (0.6 \times 10^{-6})^2$  m<sup>2</sup>/s; (b–d)  $\tau \equiv \frac{1}{2\pi f_c} = 0.0013$  s,  $\tau_0 = 0.0025$  s,  $D = 1.6452 \times 10^{-13}$  m<sup>2</sup>/s,  $A = [0.1, 0.2, 0.3] \times (0.6 \times 10^{-6})^2$  m<sup>2</sup>/s.

(3) Figure 3: (a)  $b = 1$ ,  $k = 2$ ; (b–d)  $\gamma = 1$ ,  $T_1 \equiv D_1 = 1$ ,  $\alpha \equiv \frac{T_2}{T_1} = [0.1, 0.2, 0.3]$ .



(4) Figure 4:  $E_1 = k_B T_1$ ,  $E_2 = 2k_B T_1$ ,  $\Gamma_{01} = \Gamma_{02} = \Gamma_{12} = 1 \text{ s}^{-1}$ ,  $\beta_1 = (k_B T_1)^{-1}$ ,  $T_2 = [\frac{1}{2}, \frac{1}{3}, \frac{1}{5}] \times T_1$ .

(5) Figure 6: (a)  $k_1 = 1$ ,  $k_2 = 2$ ; (b–d)  $\gamma = 1$ ,  $T_1 \equiv D_1 = 1$ ,  $\alpha \equiv \frac{T_2}{T_1} = [0.1, 0.2, 0.3]$ .

- 
- [1] C. Bustamante, J. Liphardt, and F. Ritort, The nonequilibrium thermodynamics of small systems, *Phys. Today* **58**(7), 43 (2005).
- [2] U. Seifert, Stochastic thermodynamics, fluctuation theorems and molecular machines, *Rep. Prog. Phys.* **75**, 126001 (2012).
- [3] C. Jarzynski, Equalities and inequalities: Irreversibility and the second law of thermodynamics at the nanoscale, *Annu. Rev. Condens. Matter Phys.* **2**, 329 (2011).
- [4] G. Hummer and A. Szabo, Free-energy reconstruction from nonequilibrium single-molecule pulling experiments, *Proc. Natl. Acad. Sci. USA* **98**, 3658 (2001).
- [5] J. Liphardt, S. Dumont, S. B. Smith, I. Tinoco, Jr., and C. Bustamante, Equilibrium information from nonequilibrium measurements in an experimental test of Jarzynski's equality, *Science* **296**, 1832 (2002).
- [6] G. Verley, M. Esposito, T. Willaert, and C. Van den Broeck, The unlikely Carnot efficiency, *Nat. Commun.* **5**, 4721 (2014).
- [7] G. Verley, T. Willaert, C. Van den Broeck, and M. Esposito, Universal theory of efficiency fluctuations, *Phys. Rev. E* **90**, 052145 (2014).
- [8] S. K. Manikandan, L. Dabelow, R. Eichhorn, and S. Krishnamurthy, Efficiency Fluctuations in Microscopic Machines, *Phys. Rev. Lett.* **122**, 140601 (2019).
- [9] T. R. Gingrich, J. M. Horowitz, N. Perunov, and J. L. England, Dissipation Bounds All Steady-State Current Fluctuations, *Phys. Rev. Lett.* **116**, 120601 (2016).
- [10] P. Pietzonka, A. C. Barato, and U. Seifert, Universal bounds on current fluctuations, *Phys. Rev. E* **93**, 052145 (2016).
- [11] J. M. Horowitz and T. R. Gingrich, Proof of the finite-time thermodynamic uncertainty relation for steady-state currents, *Phys. Rev. E* **96**, 020103(R) (2017).
- [12] A. C. Barato and U. Seifert, Thermodynamic Uncertainty Relation for Biomolecular Processes, *Phys. Rev. Lett.* **114**, 158101 (2015).
- [13] J. M. Horowitz and T. R. Gingrich, Thermodynamic uncertainty relations constrain nonequilibrium fluctuations, *Nat. Phys.* **16**, 15 (2020).
- [14] U. Seifert, From stochastic thermodynamics to thermodynamic inference, *Annu. Rev. Condens. Matter Phys.* **10**, 171 (2019).
- [15] R. S. Ellis, *Entropy, Large Deviations, and Statistical Mechanics* (Taylor & Francis, Oxford, UK, 2006), Vol. 1431.
- [16] H. Touchette, The large deviation approach to statistical mechanics, *Phys. Rep.* **478**, 1 (2009).
- [17] J. L. Lebowitz and H. Spohn, A Gallavotti–Cohen-type symmetry in the large deviation functional for stochastic dynamics, *J. Stat. Phys.* **95**, 333 (1999).
- [18] B. Derrida and J. L. Lebowitz, Exact Large Deviation Function in the Asymmetric Exclusion Process, *Phys. Rev. Lett.* **80**, 209 (1998).
- [19] R. Chetrite and H. Touchette, Nonequilibrium Markov processes conditioned on large deviations, in *Annales Henri Poincaré* (Springer, Berlin, 2015), Vol. 16, pp. 2005–2057
- [20] J. Mehl, T. Speck, and U. Seifert, Large deviation function for entropy production in driven one-dimensional systems, *Phys. Rev. E* **78**, 011123 (2008).
- [21] T. Speck, A. Engel, and U. Seifert, The large deviation function for entropy production: The optimal trajectory and the role of fluctuations, *J. Stat. Mech.: Theory Exp.* (2012) P12001.
- [22] A. Kundu, S. Sabhapandit, and A. Dhar, Large deviations of heat flow in harmonic chains, *J. Stat. Mech.: Theory Exp.* (2011) P03007.
- [23] S. Sabhapandit, Heat and work fluctuations for a harmonic oscillator, *Phys. Rev. E* **85**, 021108 (2012).
- [24] G. Verley, C. Van den Broeck, and M. Esposito, Work statistics in stochastically driven systems, *New J. Phys.* **16**, 095001 (2014).
- [25] W. A. M. Morgado and S. M. Duarte Queirós, Thermostatistics of small nonlinear systems: Gaussian thermal bath, *Phys. Rev. E* **90**, 022110 (2014).
- [26] K. Saito and A. Dhar, Waiting for rare entropic fluctuations, *Europhys. Lett.* **114**, 50004 (2016).
- [27] J. P. Garrahan, Simple bounds on fluctuations and uncertainty relations for first-passage times of counting observables, *Phys. Rev. E* **95**, 032134 (2017).
- [28] P. Singh and A. Kundu, Generalized arcsine laws for run-and-tumble particle in one dimension, *J. Stat. Mech.: Theory Exp.* (2019) 083205.
- [29] T. Bodineau and B. Derrida, Current Fluctuations in Nonequilibrium Diffusive Systems: An Additivity Principle, *Phys. Rev. Lett.* **92**, 180601 (2004).
- [30] B. Derrida, Non-equilibrium steady states: Fluctuations and large deviations of the density and of the current, *J. Stat. Mech.: Theory Exp.* (2007) P07023.
- [31] A. C. Barato, É. Roldán, I. A. Martínez, and S. Pigolotti, Arcsine Laws in Stochastic Thermodynamics, *Phys. Rev. Lett.* **121**, 090601 (2018).
- [32] P. Lévy, Sur certains processus stochastiques homogènes, *Compos. Math.* **7**, 283 (1940).
- [33] S. K. Manikandan, D. Gupta, and S. Krishnamurthy, Inferring Entropy Production from Short Experiments, *Phys. Rev. Lett.* **124**, 120603 (2020).
- [34] S. Otsubo, S. Ito, A. Dechant, and T. Sagawa, Estimating entropy production by machine learning of short-time fluctuating currents, *Phys. Rev. E* **101**, 062106 (2020).
- [35] T. Van Vu, V. T. Vo, and Y. Hasegawa, Entropy production estimation with optimal current, *Phys. Rev. E* **101**, 042138 (2020).
- [36] S. K. Manikandan, S. Ghosh, A. Kundu, B. Das, V. Agrawal, D. Mitra, A. Banerjee, and S. Krishnamurthy, Quantitative analysis of nonequilibrium systems from short-time experimental data, *Commun. Phys.* **4**, 258 (2021).
- [37] S. Otsubo, S. K. Manikandan, T. Sagawa, and S. Krishnamurthy, Estimating entropy production along a single nonequilibrium trajectory, *Commun. Phys.* **5**, 11 (2022).
- [38] R. L. Jack, Ergodicity and large deviations in physical systems with stochastic dynamics, *Eur. Phys. J. B* **93**, 74 (2020).
- [39] U. Seifert, Entropy Production Along a Stochastic Trajectory and An Integral Fluctuation Theorem, *Phys. Rev. Lett.* **95**, 040602 (2005).

- [40] N. Merhav and Y. Kafri, Statistical properties of entropy production derived from fluctuation theorems, *J. Stat. Mech.: Theory Exp.* (2010) P12022.
- [41] P. Pietzonka, F. Ritort, and U. Seifert, Finite-time generalization of the thermodynamic uncertainty relation, *Phys. Rev. E* **96**, 012101 (2017).
- [42] A. Dechant and S.-i. Sasa, Current fluctuations and transport efficiency for general Langevin systems, *J. Stat. Mech.: Theory Exp.* (2018) 063209.
- [43] Y. Hasegawa and T. Van Vu, Fluctuation Theorem Uncertainty Relation, *Phys. Rev. Lett.* **123**, 110602 (2019).
- [44] I. Neri, E. Roldán, and F. Jülicher, Statistics of Infima and Stopping Times of Entropy Production and Applications to Active Molecular Processes, *Phys. Rev. X* **7**, 011019 (2017).
- [45] S. Pigolotti, I. Neri, E. Roldán, and F. Jülicher, Generic Properties of Stochastic Entropy Production, *Phys. Rev. Lett.* **119**, 140604 (2017).
- [46] F. Mori, S. N. Majumdar, and G. Schehr, Distribution of the time of the maximum for stationary processes, *Europhys. Lett.* **135**, 30003 (2021).
- [47] T. R. Gingrich and J. M. Horowitz, Fundamental Bounds on First Passage Time Fluctuations for Currents, *Phys. Rev. Lett.* **119**, 170601 (2017).
- [48] Note Marcinkiewicz theorem [76], which implies that if a distribution is not Gaussian, then it will have further nonzero cumulants.
- [49] J. R. Gomez-Solano, L. Bellon, A. Petrosyan, and S. Ciliberto, Steady-state fluctuation relations for systems driven by an external random force, *Europhys. Lett.* **89**, 60003 (2010).
- [50] A. Pal and S. Sabhapandit, Work fluctuations for a Brownian particle in a harmonic trap with fluctuating locations, *Phys. Rev. E* **87**, 022138 (2013).
- [51] S. K. Manikandan and S. Krishnamurthy, Asymptotics of work distributions in a stochastically driven system, *Eur. Phys. J. B* **90**, 258 (2017).
- [52] S. K. Manikandan and S. Krishnamurthy, Exact results for the finite time thermodynamic uncertainty relation, *J. Phys. A: Math. Theor.* **51**, 11LT01 (2018).
- [53] See Eq. (14b) in Ref. [36] for the choice of  $c_i$ 's that define  $J = \Delta S_{\text{tot}}$ .
- [54] The exact analytic calculation involves the computation of the finite-time moment generating function  $G(\lambda) = \langle e^{-\lambda \Delta S_{\text{tot}}} \rangle_t$ , using a path integral technique which was developed in Ref. [51] and used in Ref. [52]. For completeness, we reproduce the results (from Ref. [52]) in Appendix A.
- [55] S. Bera, S. Paul, R. Singh, D. Ghosh, A. Kundu, R. Banerjee, and A. Adhikari, Fast Bayesian inference of optical trap stiffness and particle diffusion, *Sci. Rep.* **7**, 41638 (2017).
- [56] Parameters used in the plots are given in Appendix D.
- [57] B. Das, S. K. Manikandan, and A. Banerjee, Inferring entropy production in anharmonic Brownian gyrators, [arXiv:2204.09283](https://arxiv.org/abs/2204.09283) (2022).
- [58] H. E. D. Scovil and E. O. Schulz-DuBois, Three-Level Masers as Heat Engines, *Phys. Rev. Lett.* **2**, 262 (1959).
- [59] Y. Zou, Y. Jiang, Y. Mei, X. Guo, and S. Du, Quantum Heat Engine Using Electromagnetically Induced Transparency, *Phys. Rev. Lett.* **119**, 050602 (2017).
- [60] J. Klatzow, J. N. Becker, P. M. Ledingham, C. Weinzetl, K. T. Kaczmarek, D. J. Saunders, J. Nunn, I. A. Walmsley, R. Uzdin, and E. Poem, Experimental Demonstration of Quantum Effects in The operation of Microscopic Heat Engines, *Phys. Rev. Lett.* **122**, 110601 (2019).
- [61] T. Van Vu and K. Saito, Thermodynamics of Precision in Markovian Open Quantum Dynamics, *Phys. Rev. Lett.* **128**, 140602 (2022).
- [62] V. Singh, Optimal operation of a three-level quantum heat engine and universal nature of efficiency, *Phys. Rev. Res.* **2**, 043187 (2020).
- [63] S. K. Manikandan, Equidistant quenches in few-level quantum systems, *Phys. Rev. Res.* **3**, 043108 (2021).
- [64] G. Milburn, The thermodynamics of clocks, *Contemp. Phys.* **61**, 69 (2020).
- [65] See discussion around Eq. (92) in Ref. [64].
- [66] P. T. von Hippel, Mean, median, and skew: Correcting a textbook rule, *J. Stat. Edu.* **13** (2005).
- [67] R. D. Vale and R. J. Fletterick, The design plan of kinesin motors, *Annu. Rev. Cell Dev. Biol.* **13**, 745 (1997).
- [68] M. J. Schnitzer and S. M. Block, Kinesin hydrolyses one ATP per 8-nm step, *Nature (London)* **388**, 386 (1997).
- [69] T. Ariga, M. Tomishige, and D. Mizuno, Nonequilibrium Energetics of Molecular Motor Kinesin, *Phys. Rev. Lett.* **121**, 218101 (2018).
- [70] V. Blickle and C. Bechinger, Realization of a micrometer-sized stochastic heat engine, *Nat. Phys.* **8**, 143 (2012).
- [71] I. A. Martínez, É. Roldán, L. Dinis, D. Petrov, J. M. Parrondo, and R. A. Rica, Brownian Carnot engine, *Nat. Phys.* **12**, 67 (2016).
- [72] R. Filliger and P. Reimann, Brownian Gyrotor: A Minimal Heat Engine on the Nanoscale, *Phys. Rev. Lett.* **99**, 230602 (2007).
- [73] K.-H. Chiang, C.-L. Lee, P.-Y. Lai, and Y.-F. Chen, Electrical autonomous Brownian gyrotor, *Phys. Rev. E* **96**, 032123 (2017).
- [74] H. Chang, C.-L. Lee, P.-Y. Lai, and Y.-F. Chen, Autonomous Brownian gyrators: A study on gyrating characteristics, *Phys. Rev. E* **103**, 022128 (2021).
- [75] A. Argun, J. Soni, L. Dabelow, S. Bo, G. Pesce, R. Eichhorn, and G. Volpe, Experimental realization of a minimal microscopic heat engine, *Phys. Rev. E* **96**, 052106 (2017).
- [76] J. Marcinkiewicz, Sur une propriété de la loi de gauss, *Math. Z.* **44**, 612 (1939).
- [77] J. Li, J. M. Horowitz, T. R. Gingrich, and N. Fakhri, Quantifying dissipation using fluctuating currents, *Nat. Commun.* **10**, 1666 (2019).
- [78] M. Chaichian and A. Demichev, *Path Integrals in Physics, Volume I: Stochastic Processes and Quantum Mechanics* (CRC Press, Boca Raton, FL, 2018).
- [79] K. Kirsten and A. J. McKane, Functional determinants by contour integration methods, *Ann. Phys.* **308**, 502 (2003).
- [80] The entropy currents of the gyrotor with harmonic potential, where the dynamical equations are linear, can be identified using standard approaches [36,75,77]. However the entropy currents for the anharmonic gyrators is nontrivial to find analytically due to indelible nonlinearities present in the governing dynamical equation. To overcome this difficulty we use the short-time inference scheme [57].
- [81] <https://doi.org/10.6084/m9.gshare.17703269.v2>.
- [82] Wolfram Research, ContinuousMarkovProcess—Wolfram Language Documentation (2012), <https://reference.wolfram.com/language/ref/ContinuousMarkovProcess.html>.